Geophys. J. R. astr. Soc. (1987) **90**, 369–374

Fractal structure of spatial distribution of microfracturing in rock

Takayuki Hirata *Department of Geophysics, Faculty of Science, Kyoto University, Sakyo, Kyoto 606, Japan*

Takashi Satoh *Geological Survey of Japan, Yatabe, Ibaragi 305, Japan*

Keisuke Ito *Department of Earth Sciences, Faculty of Science, Kobe University, Nada, Kobe 657, Japan*

Accepted 1987 January 6. Received 1987 January 6; in original form 1986 July 31

Summary. A constant stress fracture experiment of Oshima granite was carried out at the confining pressure of 40 MPa. Hypocentres of 2064 acoustic emissions were located during the experiment. Using the 'correlation integral', we found that the spatial distribution of hypocentres of acoustic emission is a fractal, and that the fractal dimension decreases with the evolution of rock fracturing. The spatial distribution of earthquake's hypocentres reveals fractals ranging from regional to worldwide distribution. If we extrapolate from laboratory measurements, it is possible to predict the occurrence of large earthquakes by the decrease in the fractal dimension.

Key words: fractal, fractal dimension, stochastic self-similarity, microfracturing, spatial distribution, creep

Introduction

Fractal is a general concept for self-similarity introduced by Mandelbrot (1983), who took the term 'fractal' from the Latin fractus, which describes the appearance of a broken stone: irregular and fragmented. Actually, many natural rock surfaces are scaling, which are literally fractal. Brown & Scholz (1985) showed that the geometry of the fracture surface of rocks, e.g. joints and faults, is a fractal. In his early study on fractal geometry, Mandelbrot (1967) showed that a coastline, which is a large rock surface, is also a fractal. If natural rock surfaces are generated by superposition of the fracture process of rocks, we can expect the fracture process of rocks to be a fractal (Mandelbrot 1983).

The fracture process of a rock, including earthquakes, produces some fractal structures. The Gutenberg–Richter relationship indicates a self-similarity in frequency–magnitude and is apparently valid for various fracture scales from microcracking of rocks to large earth-

quakes (Mogi 1962; Aki 1981; King 1983). Kagan & Knopoff (1978, 1981) demonstrated that the time series of the seismic process is also fractal; if every earthquake is regarded as a multishock event, the rate of occurrence of dependent shocks on the occurrence of the mainshock increases with t^{-1}, where t is the time from the origin time of the main shock. By using correlation functions, Kagan & Knopoff (1980) showed that the spatial distributions of earthquake epicentres have stochastic self-similarities and that the fractal dimension changes from 1 to 1.5 with the hypocentral depth. Using a box-counting algorithm, Sadovskiy *et al.* (1984) demonstrated that the spatial distribution of both the earthquakes on a worldwide scale and in the local Nurek-region earthquakes is fractal. The fractal dimensions of earthquakes on a worldwide scale and in the Nurek-region local catalogue are 1.6 and 1.4, respectively. The box-counting method ignores the heterogeneous distribution of a fractal set and therefore gives (in principle) a greater fractal dimension than the correlation integral method (Grassberger 1983). The spatial distribution of earthquakes is also fractal. If the processes microfracturing and earthquakes are related, one can ask if the microfractures also display this fractal behaviour? Hypocentres of acoustic emission were located in the laboratory rock-fracture experiment, and examined to discover whether or not the spatial distribution of microfracturing is a fractal.

Rock fracture experiment

We carried out a constant-stress fracture experiment of Oshima granite under a confining pressure of 40 MPa. The differential stress was held constant at 547 MPa, which was about 85 per cent of the fracture strength obtained in a constant stress-rate fracture test of about 2×10^{-1} MPa s^{-1}. Fluctuations of the axial stress and the confining pressure during the creep were controlled to less than ±0.1 and ±0.2 per cent, respectively. The rock specimen was a

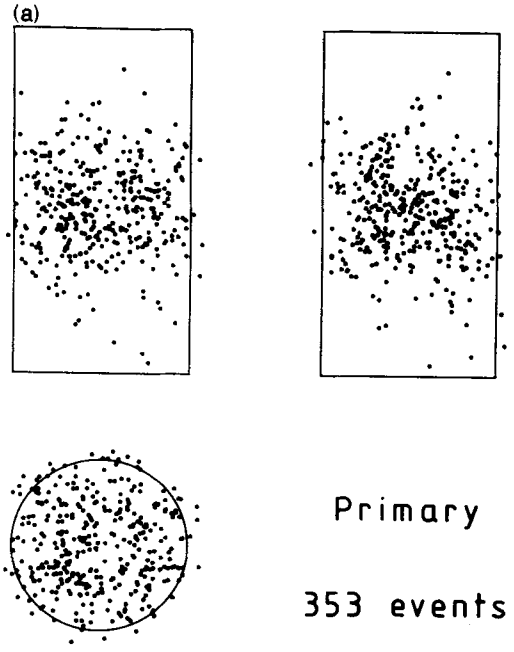

Figure 1. Orthographic projections of acoustic emission hypocentres. Hypocentres of (a) 353, (b) 273 and (c) 1438 events were determined during the primary, secondary and tertiary creep, respectively.

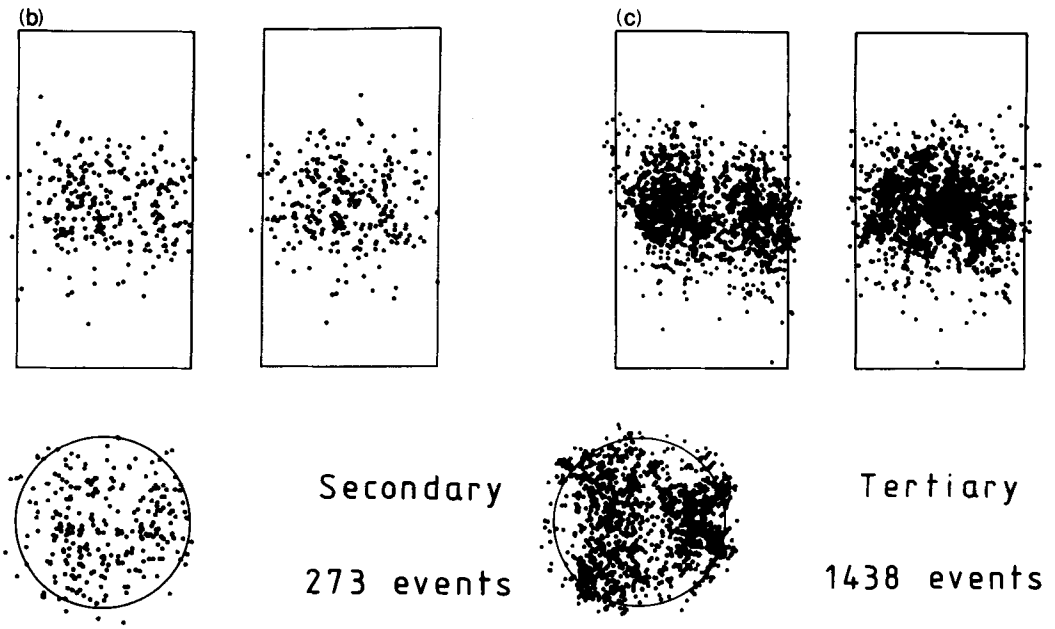

Figure 1–*continued*

cylinder 50 mm in diameter and 100 mm long. The parallelism between the ends was set to within ±0.005 mm. After vacuum drying, the specimen was kept at room environment over 2 months prior to the experiments.

When a rock is stressed, elastic waves called acoustic emissions are generated by microfracturing. These acoustic emissions were detected by 20 PZT transducers (resonant frequency is 2 MHz) mounted on the rock specimen. To eliminate the effects of the anisotropy of *P*-wave velocity in stressed rock for hypocentre locations, we measured the *P*-wave velocity both parallel and perpendicular to the loading axis during the experiment and used these velocities for determination of hypocentres. Using arrival times at each transducer, the hypocentre of acoustic emission was determined by basically the same algorithm used for determination of an earthquake's hypocentre (Nishizawa, Onai & Kusunose 1984; Yanagidani *et al.* 1985).

Hypocentres of 2064 acoustic emission events were located during the creep. The accuracy of determination of acoustic emission hypocentres was within ±2 mm. Fig. 1 (a, b, c) (respectively) shows the hypocentre distributions of acoustic emission at the so-called primary or transient creep (0–4410 s), the secondary or stationary creep (4410–15 210 s) and the tertiary creep (15 210–22 410 s) which is an accelerating stage leading to failure. The stages of creep are determined from the time versus strain relation shown in Fig. 2.

Correlation integral

The correlation integrals $C(r)$ for the hypocentre distributions $(p_1, p_2, \ldots, p_N)$ shown in Fig. 1 were calculated in three dimensions. They are given by

$$C(r) = \frac{2}{N(N-1)} Nr(R < r), \tag{1}$$

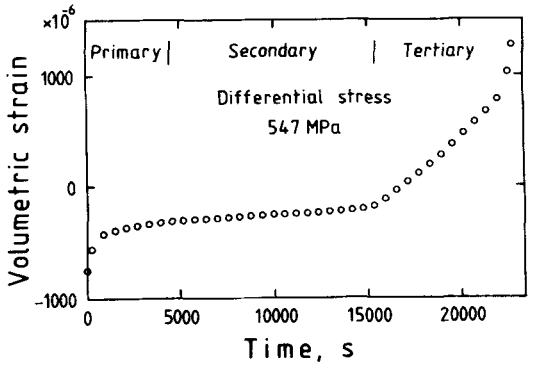

Figure 2. Time versus average volumetric strain during the creep. Strains were measured with six strain gauges mounted on the centre of the specimen at 60° intervals.

where $Nr(R < r)$ is the number of pairs (p_i, p_j) with a distance smaller than r, and N is 353, 273 and 1438 for the primary, secondary and tertiary creep, respectively. If the distribution has a fractal structure, $C(r)$ is expressed by

$$C(r) \propto r^D, \tag{2}$$

where D is a kind of fractal dimension called the correlation exponent (Grassberger 1983) that gives the lower limit of the Hausdorff dimension. We can estimate the fractal dimension using a box-counting algorithm, but the estimation is unstable depending on the location and size of the boxes when the number of data is small. This alternative method can be used even for a small number of data.

The correlation integrals versus the distance for the hypocentre distribution at each stage of creep is plotted on a double logarithmic scale in Fig. 3. The actual data fall on the straight lines, which indicate that the spatial distributions of acoustic emission have fractal structures. The fractal dimension estimated from the slope was 2.75, 2.66 and 2.25 at the stages of primary creep, secondary creep and tertiary creep, respectively.

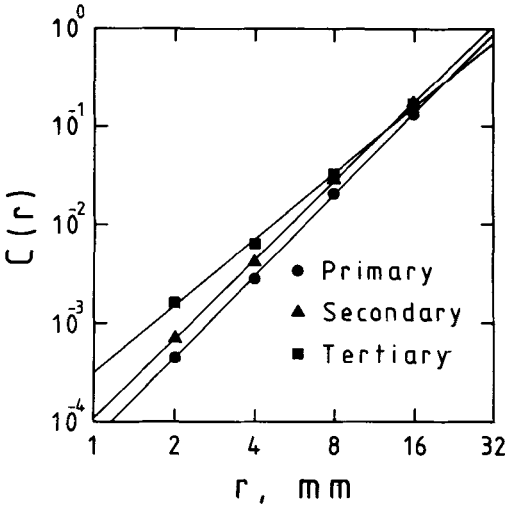

Figure 3. Correlation integral versus distance for each stage of the creep. Fractal dimensions are 2.75, 2.66 and 2.25, for the primary, secondary and tertiary creep, respectively.

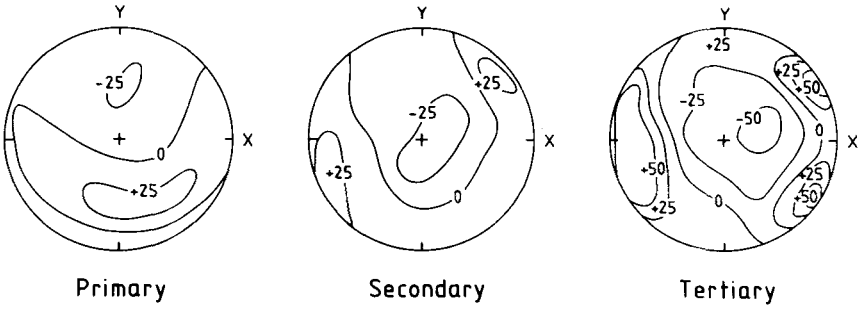

Figure 4. Distribution of the orientations of the hypocentre pairs (p_i, p_j). An upper hemisphere of equal-area projection has been used for the directions of the pairs. The values on contour lines are the deviation from the averaged density normalized as 100.

The hypocentre pair of (p_i, p_j) forms a vector. The distribution of the orientations of the pairs at each creep stage is shown in Fig. 4. The orientation also tends to cluster with progress of the creep; according to Fig. 4, this cluster means that the hypocentre localization is a volumetric one with some cluster centres rather than planar ones. This result coincides with the result of the uniaxial creep test of Oshima granite by Yanagidani *et al.* (1985).

Discussion

If hypocentres are distributed at random in three dimensions, the fractal dimension D defined by (2) is 3. The decrease of the fractal dimension to less than 3 as creep progresses means that hypocentres of acoustic emission tend to cluster with a self-similar structure in space. Since the dimension of the planar section of a fractal set with fractal dimension D in 3-D space is generally $D-1$ (Mandelbrot 1983), the fractal dimension of the planar section of the acoustic emission hypocentres is between 1.75 and 1.25, roughly coinciding with the fractal dimension ($1.0 < D < 1.6$) of earthquake epicentres which occur within a plate and thus are distributed in two dimensions (Kagan & Knopoff 1980; Sadovskiy *et al.* 1984). This suggests that fracturing of rocks is a scale-invariant process from the macroscopic level of earthquakes, at least small-scale earthquakes which do not fracture the entire crust, to the microscopic level of microfracturing as proposed by other workers (Allègre, Le Mouel & Provost 1982).

The fractal dimensions obtained in the present study, Kagan & Knopoff (1980) and Sadovskiy *et al.* (1984) are one for the spatial distribution of point sources, but not for the shape of the fracture plane (Brown & Scholz 1985), nor for the size distribution of fractures which is related to b-values of earthquake magnitude–frequency relationships (Aki 1981; King 1983; Main & Burton 1984). Each fractal dimension represents a different aspect of the fractal structure of fracturing and need not be equal. In the present study, we measured the magnitude–frequency relationship, obtaining the magnitude from the maximum amplitude of acoustic emission. The relationship is expressed by $\log N(m > M) = a - bM$, where N is the total number of events of which magnitude m is greater than M. We did not observe a correlation between b and D, though b tends to decrease just before failure.

If the scale-invariant nature of fracturing holds from the microscopic level of microfracturing in rocks to the macroscopic level of earthquakes, the results of the rock fracture experiment can be extrapolated to an explanation of the natural earthquake. For example, Ouchi & Uekawa (1986) reported that the degree of clustering of earthquakes increases before large earthquakes, which is supported on a microfracturing scale by our findings. We

therefore propose that the use of the decrease in the fractal dimension of earthquake hypocentres may be valuable for predicting large earthquakes. Although b-values are also said to tend to decrease before large earthquakes, in our laboratory experiment, the fractal dimension D appeared to be more sensitive than the b-values for predicting the main fracturing. This may be due to a shortcoming in the laboratory experiment.

Acknowledgments

We thank O. Nishizawa and K. Kusunose for their assistance with the experiment and discussion. We are grateful to T. Yanagidani, N. Fujii and H. Takayasu for their comments.

References

Aki, K., 1981. A probabilistic synthesis of precursory phenomena, in *Earthquake Prediction*, pp. 566–574, eds Simpson, D. W. & Richards, P. G., American Geophysical Union, Washington, DC.

Allègre, C. J., Le Mouel, J. L. & Provost, A., 1982. Scaling rules in rock fracture and possible implications for earthquake prediction, *Nature*, **297**, 47–49.

Brown, S. R. & Scholz, C. H., 1985. Broad bandwidth study of the topography of natural rock surfaces, *J. geophys. Res.*, **90**, 12 575–12 582.

Grassberger, P., 1983. Generalized dimensions of strange attractors, *Phys. Lett.*, **97**, 227–230.

Kagan, Y. Y. & Knopoff, L., 1978. Statistical study of the occurrence of shallow earthquakes, *Geophys. J. R. astr. Soc.*, **55**, 67–86.

Kagan, Y. Y. & Knopoff, L., 1980. Spatial distribution of earthquakes: the two-point correlation function, *Geophys. J. R. astr. Soc.*, **62**, 303–320.

Kagan, Y. Y. & Knopoff, L., 1981. Stochastic synthesis of earthquake catalogs, *J. geophys. Res.*, **86**, 2853–2862.

King, G., 1983. The accommodation of large strains in the upper lithosphere of the earth and other solids by self-similar fault systems: the geometrical origin of b-value, *Pure appl. Geophys.*, **121**, 761–815.

Main, I. G. & Burton, P. W., 1984. Information theory and the earthquake frequency-magnitude distribution, *Bull. seism. Soc. Am.*, **74**, 1409–1426.

Mandelbrot, B. B., 1967. How long is the coast of Britain?, *Science*, **155**, 636–638.

Mandelbrot, B. B., 1983. *The Fractal Geometry of Nature*, Freeman, New York.

Mogi, K., 1962. Magnitude–frequency relation for elastic shocks accompanying fractures of various materials and some related problems in earthquakes, *Bull. Earthq. Res. Inst. Tokyo Univ.*, **40**, 831–853.

Nishizawa, O., Onai, K. & Kusunose, K., 1984/1985. Hypocenter distribution and focal mechanism of AE events during two stress stage creep in Yugawara andesite, *Pure appl. Geophys.*, **122**, 36–52.

Ouchi, T. & Uekawa, T., 1986. Statistical analysis of the spatial distribution of earthquakes – variation of the spatial distribution of earthquakes before and after large earthquakes, *Phys. Earth planet. Int.*, **44**, 211–225.

Sadovskiy, M. A., Golubeva, T. V., Pisarenko, V. F. & Shnirman, M. G., 1984. Characteristic dimensions of rock and hierarchical properties of seismicity, *Izvestiya, Earth Phys.*, **20**, 87–96.

Yanagidani, T., Ehara, S., Nishizawa, O., Kusunose, K. & Terada, M., 1985. Localization of dilatancy in Ohshima granite under constant uniaxial stress, *J. geophys. Res.*, **90**, 6840–6858.